Evolution of mixing width induced by general Rayleigh-Taylor instability

You-sheng Zhang,[1] Zhi-wei He,[1] Fu-jie Gao,[1] Xin-liang Li,[2] and Bao-lin Tian[1,*]

[1] *Key Laboratory of Computational Physics, Institute of Applied Physics and Computational Mathematics, Beijing 100094, China*

[2] *Institute of Mechanics, Chinese Academy of Sciences, Beijing 100190, China*

(Received 12 January 2016; published 6 June 2016)

Turbulent mixing induced by Rayleigh-Taylor (RT) instability occurs ubiquitously in many natural phenomena and engineering applications. As the simplest and primary descriptor of the mixing process, the evolution of mixing width of the mixing zone plays a notable role in the flows. The flows generally involve complex varying acceleration histories and widely varying density ratios, two dominant factors affecting the evolution of mixing width. However, no satisfactory theory for predicting the evolution has yet been established. Here a theory determining the evolution of mixing width in general RT flows is established to reproduce, first, all of the documented experiments conducted for diverse (i.e., constant, impulsive, oscillating, decreasing, increasing, and complex) acceleration histories and all density ratios. The theory is established in terms of the conservation principle, with special consideration given to the asymmetry of the volume-averaged density fields occurring in actual flows. The results reveal the sensitivity or insensitivity of the evolution of a mixing front of a neighboring light or heavy fluid to the degree of asymmetry and thus explain the distinct evolutions in two experiments with the same configurations.

DOI: 10.1103/PhysRevE.93.063102

I. INTRODUCTION

As shown in Fig. 1, when two fluids of density ρ_i ($i = 1 =$ light, $i = 2 =$ heavy) are separated by a perturbed interface and are accelerated in the direction opposite to that of the density gradient, Rayleigh-Taylor (RT) instability occurs and develops into turbulent mixing zones consisting of a bubble mixing zone (BMZ, formed when a light fluid penetrates a heavy fluid) and a spike mixing zone (SMZ, formed when a heavy fluid penetrates a light fluid) [1]. The mixing is a process by which two separated fluids of different densities seek to reduce their combined potential energy [2] and occurs ubiquitously [3] in systems extending from the micro- [3] to astrophysical [4] scales. As the simplest and primary descriptor of the mixing process, the location of the two edges of the mixing zone [i.e., mixing width $h_i(t)$, $i = 1 =$ spikes, $i = 2 =$ bubbles] plays a notable role [1] in many natural phenomena (e.g., supernova explosions [5]) and engineering applications (e.g., inertial confinement fusion [6]). The scenarios generally involve complex varying acceleration histories $g(t)$ and widely varying density ratios $R \equiv \rho_2/\rho_1$, two dominant factors affecting the evolution of $h_i(t)$ in the turbulent regime [7].

To predict the evolution of $h_i(t)$ in the general RT problems, many models have been developed over the last few decades, such as the bubble-competition model [8], energy-transfer model [9], stationary-centroid model [10], and buoyancy-drag models [1,7,11–13]. However, no model has completely [7] reproduced the experimental observed $h_i(t)$ [12,14–16]. In fact, even for the simplest RT problem with a constant acceleration, i.e., $g = g_0$, previous models do not give satisfactory predictions. For example, the models produced only one pair of quadratic growth coefficients $\alpha_i^A \equiv h_i/(Agt^2)$, while few pairs of α_i^A were observed [12] (see Fig. 2), where $A \equiv (R-1)/(R+1) \in (0,1)$ is the Atwood number.

*tian_baolin@iapcm.ac.cn

In this paper, we describe a theory for the general incompressible RT problem in an attempt to understand the problem. This theory is established in terms of the conservation principle, with special consideration given to the asymmetry of the volume-averaged density fields to highlight the actual flows occurring in nature. The theory is validated by the series of experiments [12,15,16]. Furthermore, it reveals that the evolution of $h_i(t)$ may be affected by initial perturbations, fluid properties, and degree of asymmetry, but governed essentially by mass, momentum conservation, and Newton's second law.

II. RESULTS

A. Theory

In this section, we establish our theory by referring to the configuration and notations shown in Fig. 1. In Fig. 1, $o - xyz$ is a noninertial reference frame fixed at the initially unperturbed interface [12], denoted by subscript 0. The acceleration is directed along the y axis with $\ddot{y} = g(t)$, where the dot denotes the time derivative. Mixing is assumed to be statistically homogeneous in the x and z directions [7,10], with the cross-sectional area set to unity. Therefore, all of the ensemble-averaged quantities depend only on y and t. The h_i quantifies the distance of the interface to the mixing fronts, defined by the locations with concentration $c = 1\%(99\%)$ [17]. $V(y)$ quantifies the propagation speed of an iso-concentration surface [10] at y, with $V(h_i) \equiv v_i \equiv \dot{h}_i$. Here $\bar{f} \equiv [\int_0^{h_i} f(y_i)\,dy_i]/h_i$ essentially defines a volume average in SMZs and BMZs. From the left to the right, the flow fields consist of a pure light fluid zone with density ρ_1, a SMZ and BMZ with an average density $\bar{\rho}_1$ and $\bar{\rho}_2$, and a pure heavy fluid zone with density ρ_2. For the investigated RT problem, the density profile increases monotonically from ρ_1 of the light fluid, to ρ_0 at the interface, and to ρ_2 of the heavy fluid, leading to $\bar{\rho}_i = w_i\rho_0 + (1 - w_i)\rho_i$, where w_i is positive and is named as mixing weight. Obviously w_i should be less than the 1/2 of the mixing weight of the linearly varying

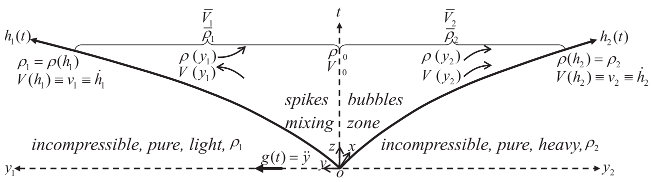

FIG. 1. Configuration and notations for the currently investigated Rayleigh-Taylor problem.

density profile since $\rho(y_i)$ transitions smoothly near h_i. With the aid of w_i, now we define the symmetry or asymmetry of volumed-averaged density fields for the currently investigated problem: density fields in BMZ and SMZ are said to be in symmetry (asymmetry) if the symmetry factor $\eta \equiv w_1/w_2 = (\neq)1$. Based on this definition, we established our theory with conservation principles, as follows.

First, the conservation of mass [7] requires

$$\rho_1 h_1 + \rho_2 h_2 = \bar{\rho}_1 h_1 + \bar{\rho}_2 h_2. \tag{1}$$

Second, given the success of the momentum-driven viewpoint [18] in understanding RT mixing and that of the stationary centroid hypothesis in predicting $h_i(t)$ of constant acceleration RT problems [7,10,19], it seems plausible for an approximation of the vanishing resultant force on the entire mixing region, resulting in the quasiconservation of momentum (similar to the stationary centroid hypothesis [7,10,19]):

$$\bar{\rho}_1 h_1 \dot{\bar{V}}_1 = \bar{\rho}_2 h_2 \dot{\bar{V}}_2, \tag{2}$$

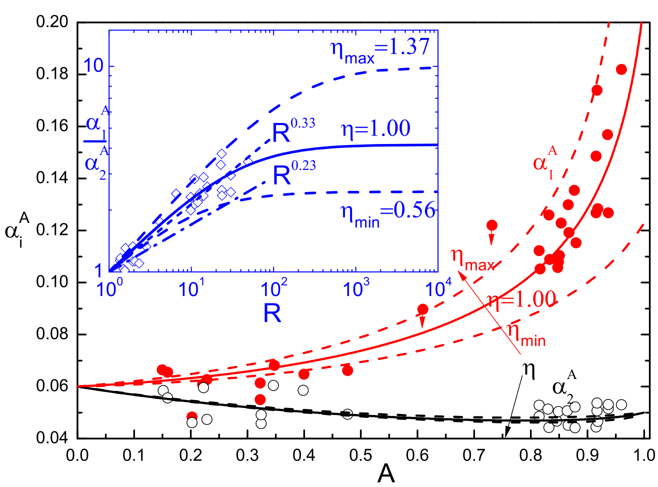

FIG. 2. Validation of current theory for problems with constant acceleration and at all density ratios. The lines show the variations of the predicted quadratic growth coefficients α_1^A (red, upper),α_2^A (black, lower), and its ratio α_1^A/α_2^A (blue, inset) [see Eq. (A1) for the analytical expression] with A, or equivalently R. The symbols show the experimental results [12], and the two points with $\downarrow$ denote overmeasured data [12]. In the predictions, different values of η are used to reveal the dependence of the evolutions on the degree of asymmetry, to reproduce the many observed pairs of α_i^A at the same R, and to explain the distinct difference between the empirical formula of $\alpha_1^A/\alpha_2^A \sim R^{0.33}$ (short dashed line) observed in linear electric motor experiments [12] (open diamonds) and that of $\alpha_1^A/\alpha_2^A \sim R^{0.23}$ (dash-dot line) in rocket-rig experiments [14,20] (see the references for the experimental data).

which is established by regarding the BMZ (SMZ) as a particle. Equation (2) implies that the evolutions of $h_1(t)$ and $h_2(t)$ depend on each other and thus should not be predicted with the two independent equations of the previous models [1,7,11–13]. Consequently one additional evolution equation is needed only. Given that the bubble structure is independent of the density ratio R [8], we prefer to establish an evolution equation for $h_2(t)$ to avoid R-dependent parameters. For BMZ, it incurs three forces, namely, a buoyancy force $f_b = \rho_2 h_2 g(t)$, an inertial force $f_i = \bar{\rho}_2 h_2 g(t)$, and a drag force $f_d = C_d \rho_2 v_2 |v_2|$ [7], where C_d is the drag coefficient. Applying Newton's second law to BMZ gives

$$\bar{\rho}_2 h_2 \dot{\bar{V}}_2 = f_b - f_i - f_d. \tag{3}$$

In Eqs. (2) and (3), instead of using the local speed of advance of the mixing fronts (i.e., v_i) to quantify the rate of change of the momentum in previous models [1,7,11–13], the volume-averaged speed of advance of BMZ and SMZ (i.e., $\bar{V}_i$) is used in the current theory. This is more reasonable in physics since the entire BMZ is regarded as being a particle, such that $\bar{V}_2$ should be used. Due to this, however, Eqs. (1) to (3) become unclosed, such that an assumption, with which the relationship between $\bar{V}_i$ and v_i can be derived, is needed. We notice that a reasonable assumption should meet the two following physical intuitions: (1) For unity R, due to symmetry, $V(y_i)$ should increase monotonically from 0 at $y = 0$ to $V(h_i)$ at $y = h_i$; (2) for any value of R, due to continuity, $(dV/dy)|_{y\to 0^+} = (dV/dy)|_{y\to 0^-}$. Therefore, the simplest physical assumption is the parabolic velocity profile of $V(y_i)/V(h_i) = (y_i/h_i)^2$. The assumption gives $\bar{V}_i = v_i/3$, with which the rearrangement [7] of Eqs. (1) to (3) yields the final evolution equation:

$$\gamma\chi\dot{v}_1 = \dot{v}_2 = \beta A g(t) - C\phi v_2|v_2|/h_2, \tag{4}$$

where $\gamma \equiv \bar{\rho}_1/\bar{\rho}_2 = [(R-1)w_2\eta + (1+\chi\eta)]/\Theta$, $\chi \equiv h_1/h_2$, $\beta \equiv 3(\phi - 1)/A = 3w_2\chi\eta(R+1)/\Theta$, $C \equiv 3C_d$, $\phi \equiv \rho_2/\bar{\rho}_2 = R(1+\chi\eta)/\Theta$, and $\Theta \equiv R(1+\chi\eta) + w_2\chi\eta(1-R)$.

B. Validation

Three parameters, η, w_2, C, are incorporated into the current theory. Due to the above mentioned R-independent bubble structure, the parameters are postulated to be R-independent and are determined definitely in the Appendix. With the determined parameters, our theory is systematically validated in Figs. 2–4 for general RT mixing.

Figure 2 shows the validation for an RT problem with constant acceleration, where our predictions (see the Appendix) are in good agreement with the results of the experiments [12] regardless of the density ratio. The figure further indicates that (1) except for the two overmeasured points, almost every observed α_1^A is within the region bounded by curves with the maximum and minimum η; (2) except for very few experiments, the density fields in BMZ and SMZ are symmetrical approximately in most cases since the majority of the observed α_i^A values lie on curves for which $\eta \approx 1$; (3) $\alpha_{1(2)}^A$, or equivalently $h_{1(2)}(t)$, is closely (slightly) dependent on η, consistent with the results of the experiments; and (4) α_1^A/α_2^A is closely dependent on η, explaining the distinct observed difference [20] between the results of Young's [14] and Dimonte's [12] experiments for the first time.

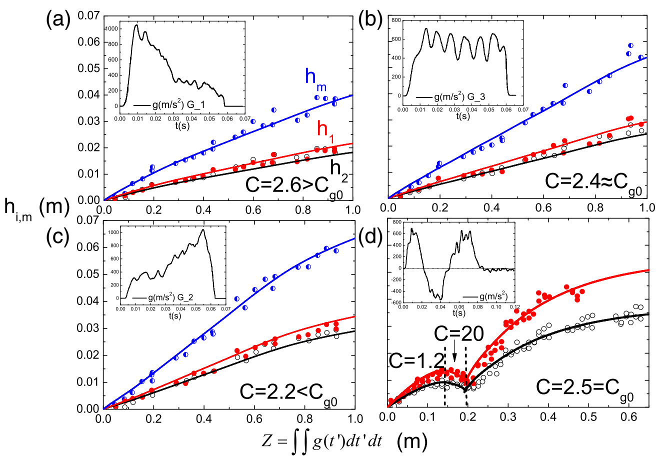

FIG. 3. Validation of the current theory for problems with variable acceleration and at different density ratios. The subfigures compare the evolutions of $h_1(t)$ (red, middle line in fipanels a–c and upper line in panel d), $h_2(t)$ (black, lower line), and $h_m(t) \equiv h_1(t) + h_2(t)$ (blue, upper line in panels a–c) for problems driven respectively by (a) decreasing (G_1 [12]), (b) oscillating (G_3 [12]), (c) increasing (G_2 [12]), and (d) sine-function-like [16] acceleration histories, as shown in the inset. $R = 1.57$ in cases a, b, c, and $R = 2.83$ in case d. The symbols show the experimental results, and the lines show the predictions for Eq. (4) with a symmetry factor $\eta = 1$, initial values of $v_{i0} = 0$ and $h_{i0} = 10^{-6}m$ [7], and the suggested C shown in the fipanels.

Figures 3–4 show a validation for problems with diverse acceleration histories and at all density ratios. For variable acceleration problems, although $C[g(t)]$ has not yet been formulated, we can still predict $h_i(t)$ with a reasonable approximation of $C = \text{const}$ (see the Appendix), either entirely or piecewise. By means of this approximation, our theory is in good agreement with the results of experiments, and much better than the theory given in Ref. [7] (illustrated by the example in the inset of Fig. 4). Furthermore, as shown in Fig. 3(d), the good agreement between experiment and prediction confirms the robustness of current theory for the problem even involving complex and negative acceleration history. In this case, different from the use of constant C in the previous buoyancy-drag model [1,7,11–13], a piecewise constant approximation of C is used, with the value determined by taking into account the following physics: (1) C should be highly dependent on the direction of mixing and (2) during the period of demixing (i.e., $v_2 < 0$), C should be much larger than the C_{g0} (see more discussion in the Appendix). With the considerations, in case d three piecewise constant of $C(v_2 > 0) = 1.2 < C_{g0}$, $C(v_2 < 0) = 20 \gg C_{g0}$ and $C(v_2 > 0) = C_{g0}$ are used successively according to the change of the sign of v_2, and the use of $C(v_2 < 0) = 20 \gg C_{g0}$ successfully captures the observed demixing induced by negative $g(t)$.

As a special example of a variable acceleration problem, the impulsive acceleration problem (Richmyer-Meshkov mixing [7,12]) is extremely important to many of the flows that occur in engineering and nature, and an in-depth analysis of the solution to Eq. (4) for this problem is necessary. To this end, we have divided the entire acceleration history into stage I with impulsive acceleration and stage II with zero acceleration [12].

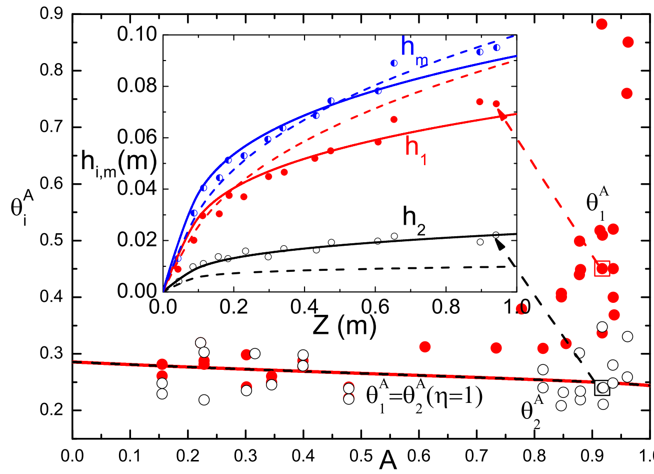

FIG. 4. Validation of current theory for problems with impulsive acceleration and at all density ratios. The symbols show the observed [12] power index θ_1^A (red, solid circle) and θ_2^A (black, hollow circle) [see Eq. (5) for the definition]. The lines of $\theta_1^A = \theta_2^A(\eta = 1)$ show the exact solution to Eq. (4) for the special initial condition of $h_{1\delta}/h_{2\delta} = v_{1\delta}/v_{2\delta} = \alpha_1^A/\alpha_2^A$ (see Sec. II). For general cases, Eq. (4) successfully reproduces all the evolutions of the impulsive experiments conducted by Dimonte [12], but only one example ($R = 23.4$,F_68,G15 [12]) is shown in the inset, which compares the results of the prediction [solid lines: Eq. (4); dashed lines: predictions by Ref. [7]] with those of the experiment [12] (symbols) for the evolutions of $h_1(t)$ (red), $h_2(t)$ (black), and $h_m(t)$ (blue). The current prediction was conducted by integrating Eq. (4) with initial values of $v_{i0} = 0$ and $h_{i0} = 10^{-6}m$ [7], experimentally measured $g(t)$ [12], and parameters η, $w_2(\eta)$, and $C_{g0}(\eta)$, where a constant $C_{g0}(\eta)$ is adopted to enable the neglect of the variation in $C[g(t)]$ during the extremely short duration of the impulsive acceleration stage I. In a very few experiments (especially those with a large R), which were probably affected by distinct initial perturbations, the density field was asymmetric, and thus η needed to be adjusted slightly around 1, as in the case of the example shown in the inset for which $\eta = 1.1$.

Given the extremely short duration of stage I, we investigated only stage II and have denoted the quantities at the end of stage I with subscript δ. For stage II with initial values of $v_{i\delta}$ and $h_{i\delta}$, Eq. (4) approximately has a power-law solution [7] of

$$h_i = h_{i\delta}\left(\frac{t}{t_{i\delta}\theta_i^A} + 1\right)^{\theta_i^A}, \quad t_{i\delta} = \frac{h_{i\delta}}{v_{i\delta}}, \theta_i^A = \theta_{i\delta}^A[1 + \varepsilon(t)], \quad (5)$$

where $\varepsilon(t)$ is generally a time-dependent small quantity (see Ref. [7] for more information).

The solution given in Eq. (5) enables us to understand some long-standing questions. First, for the special initial condition of $\chi_\delta \equiv h_{1\delta}/h_{2\delta} = v_{1\delta}/v_{2\delta} = \chi_{g_0}^A = \alpha_1^A/\alpha_2^A$, one can verify that $\varepsilon(t)$ equals zero exactly, with the corresponding power index of $\theta_1^A = \theta_2^A = \theta_{2\delta}^A(\phi)$ and $\theta_{2\delta}^A(\phi) = 1/[1 + C\phi(R,\eta,\chi_\delta)$ (see Ref. [7] for more information). In fact, substituting this exact power-law solution into the first equality of Eq. (4) yields $\gamma\chi_\delta^2 = 1$ [similar to $\gamma(\chi_{g_0}^A)^2 = 1$ obtained for problems with constant acceleration in the Appendix], from which the required special initial condition of $\chi_\delta = \chi_{g_0}^A$ is derived. This exact solution can explain the observed $\theta_1^A \approx \theta_2^A$ for $A < 0.8$ (see Fig. 4) as follows: for a problem with a small or moderate density ratio and a positive acceleration history, previous studies [12,15] suggested an empirical formula of $h_i \approx \alpha_i^A A[\int \sqrt{g(t)}\,dt]^2$, which, when applied to stage I, gives the special initial condition, leading to $\theta_1^A \approx \theta_2^A$. Second, for general cases, if $t \gg t_{i\delta}$ and we neglect the high-order modification by $\varepsilon(t)$ [7], we can obtain $\theta_2^A \approx \theta_{2\delta}^A(\phi)$ explicitly by following the procedures given by Dimonte [7], and $\theta_1^A \approx f(\chi_\delta, t_{i\delta}, \eta)$ implicitly by substituting the power-law solution into the first equality of Eq. (4). The former reveals that θ_2^A, or equivalently $h_2(t)$, is nearly independent of the initial conditions, and determined dominantly by η because $\phi(R,\eta,\chi_\delta)$ is only slightly dependent on χ_δ (this can be verified with the aid of the expression of ϕ). In contrast, the latter implies that θ_1^A, or equivalently $h_1(t)$, is sensitive to η and the initial conditions, as verified by numerical integration. These conclusions are consistent with the experimental [12] and theoretical [21] results.

III. DISCUSSION

We give some discussions on the newly defined parameters of w_2 and η involved in current theory. First, as pointed out in the beginning of the Sec. II B, the two parameters are postulated to be R-independent since the universality of bubble structure for all R. Second, according to the expression given in (A2), the w_2 depends only on η by giving α_2^0 and α_2^1 (see the next paragraph on the determination of α_2^0 and α_2^1). The mixing weight w_2 characterizes the relative mass ratio of heavy fluid to light fluid in BMZ, and it can be determined from the cross section-averaged density profile. For the problem with constant acceleration, the current theory of $w_2(\eta = 1, \alpha_2^0 = 0.06, \alpha_2^0 = 0.05) = 0.25 < 1/2$ implies that the assumption of the linearly varied averaged density profile [7] is not a good approximation, and further study of the density profile is valuable. As for the symmetry factor η, it is the unique parameter in the current theory. The η is introduced actually as a free parameter to reproduce, explain, and reveal the different evolutions in experiments using the same density ratio and acceleration history, and a strong (weak) dependence of $h_{1(2)}(t)$ on η is found. The value of η may depend on many factors and thus is sensitive in different cases. However, in the sense of statistics, we argue that η should be tend to unity and independent on R, a hypothesis coming from the random perturbations and the self-organized mixing. The good agreement of experiments and predictions shown in this paper confirms this hypothesis. Indeed, for the problem with either constant or impulsive acceleration, the good agreement of α_i^A (Fig. 2) and θ_i^A (Fig. 3) with $\eta \approx 1$ between the experiments and predictions implies that the density fields in BMZ and SMZ are symmetrically approximate in the sense of statistics. Moreover, for each specific case, the η does not equal unity exactly in most experiments. This fact implies the symmetry of the volume-averaged density fields in BMZ and SMZ would break easily in actual flows, i.e., the universality of asymmetry in nature. Although η may depend on many factors, we infer that the asymmetry of initial perturbations promise to be the most important factors. Overall,the quasisymmetry of volume-averaged density fields in SMZ and BMZ (i.e., $\eta \approx 1$) are seem to be universal in actual flows, and current work further demonstrates the success of introducing the degree of asymmetry to quantify and understand the RT problem. For other problems, the idea may work, too.

Finally, our theory was validated systematically in terms of reproducing the results of all the available experiments, but only those results obtained for systems with immiscible inviscid fluids [8,12,14,22,23] and natural perturbations [12,14,23] are presented in this paper. As is well known, however, α_2^A is highly dependent on the fluid properties (such as viscosity, miscibility) [7,17] and initial perturbations [20,24,25]. Therefore, for other systems with notably different media and/or perturbations, slightly different values of parameters α_2^0 and/or α_2^1 may be used. Nevertheless, the good agreements substantially confirm that the evolutions of general RT mixing are governed essentially by the conservation principle.

IV. CONCLUSIONS

A theory is established to predict the evolution of mixing width in general Rayleigh-Taylor flows. Different from the previous buoyancy-drag models, this theory is established by additionally considering mass and momentum conversation, by using the volumed-averaged speed of the advance of the mixing zone, by introducing a symmetry factor to highlight the property of density fields occurring in actual flows, and by assuming a parabolic-varied velocity profile. The parameters in the current theory are determined definitely by considering the asymptotic solutions. The theory is validated by the series of experiments with different acceleration histories and at any density ratios. To the best of our knowledge, this is the first time that a theory has successfully reproduced the results of all the experiments with the same parameters. The study further reveals that, besides the known dependence on fluid properties and initial perturbation, the time evolution of $h_i(t)$, especially $h_1(t)$, also depends on the symmetry factor η, but governed essentially by mass, momentum conservation, and Newton's second law.

ACKNOWLEDGMENTS

We acknowledge financial support from the Chinese Academy of Engineering Physics (CAEP) under Grant No. YZ2015015 and LCP9140C690104150C69303 and from the National Nature Science Foundation of China (NSFC) under Grants Nos. 11502029, 11572052, 11472059, 11171037, 11372330, 11472278, and 91441103.

APPENDIX: DETERMINATION OF PARAMETERS

Three parameters of η, w_2, C are determined in four steps as follows.

Step I: Obtain the exact quadratic solution of Eq. (4) for the RT problem with constant acceleration $g = g_0$. For such a problem with initial values of $h_{i0} = 0$ and $v_{i0} = 0$, we can verify that Eq, (4) can solve (see Ref. [7] for more information)

$$h_i = \alpha_i^A A g t^2, \quad \alpha_2^A = \beta/(2 + 4C_{g_0}\phi), \quad \alpha_1^A = \chi_{g_0}^A \alpha_2^A, \quad \text{(A1)}$$

where $\chi_{g_0}^A$, equivalent to α_1^A/α_2^A or h_1/h_2, are determined as follows. Substituting the quadratic solution to the first equality of Eq. (4) yields $\gamma(\chi_{g_0}^A)^2 = 1$ and then $\sum_{m=0}^{3} a_m (\chi_{g_0}^A)^m = 0$, for which the positive real root gives $\chi_{g_0}^A =$

$[B_1^{1/2}(\cos\theta+\sqrt{3}\sin\theta) \;\; -a_2]/(3a_3)$ with $a_0=-R$, $a_1=w_2\eta(R-1)-R\eta, a_2=(R-1)w_2\eta+1, a_3=\eta$, $B_1=a_2^2-3a_1a_3$, $B_2=a_1a_2-9a_0a_3$, $D=(2B_1a_2-3a_3B_2)/(2B_1^{3/2})$, and $\theta=\arccos D/3$.

Step II: Establish the algebraic interrelation between the parameters and the asymptotic quadratic-growth-coefficients with the solution obtained in step I. When $A\to 0$, we can obtain $R,\chi_{g_0}^0,\phi,\gamma\to 1$ and $\beta\to 6w_2\eta/(1+\eta)$. When $A\to 1$, we can first obtain $\chi_{g_0}^1\to[(1-w_2)\eta+\sqrt{(1-w_2)^2\eta^2+4w_2\eta}]/(2w_2\eta)$ by using $R\to\infty$ and $\gamma(\chi_{g_0}^A)^2=1$ (see step I), and then $\phi\to(1+\chi_{g_0}^1\eta)/\Psi$, $\gamma\to w_2\eta/\Psi$, $\beta\to 3w_2\chi_{g_0}^1\eta/\Psi$ with $\Psi=1+(1-w_2)\chi_{g_0}^1\eta$. Consequently, the algebraic interrelations between the parameters of η, w_2, and C and the asymptomatic quadratic growth coefficients of α_2^0, α_2^1, and α_1^1 can be obtained by substituting the above asymptotic results into the formula for α_i^A in Eq. (A1). Omitting the complex algebraic operations, we obtain finally

$$\begin{aligned}
\alpha_2^0(\eta,C_{g_0},w_2)&=6w_2\eta/[(1+\eta)(2+4C_{g_0})]\\
\alpha_2^1(\eta,C_{g_0},w_2)&=3w_2\chi_{g_0}^1\eta/[2\Psi+4C_{g_0}(1+\chi_{g_0}^1\eta)]\\
\alpha_1^1(\eta,C_{g_0},w_2)&=\alpha_2^1\chi_{g_0}^1\\
w_2(\eta,\alpha_2^0,\alpha_2^1)&=(T^2+6\eta\alpha_2^1T)/[36\eta(\alpha_2^1)^2+6\eta\alpha_2^1T]\\
C_{g_0}(\eta,\alpha_2^0,\alpha_2^1)&=3w_2\eta/[2\alpha_2^0(1+\eta)]-1/2\\
\eta(w_2,\alpha_2^0,\alpha_2^1)&=[-b_2-\sqrt{b_2^2-4b_1b_3}]/(2b_1)\\
\eta(\alpha_1^1,\alpha_2^0,\alpha_2^1)&=[-d_2-\sqrt{d_2^2-4d_1d_3}]/(2d_1),
\end{aligned}\qquad\text{(A2)}$$

where $\chi_{g_0}^1=[(1-w_2)\eta+((1-w_2)^2\eta^2+4w_2\eta)^{1/2}]/(2w_2\eta)$, $T=e_1+e_3\eta$, $b_1=e_3^2+e_2e_3(1-w_2)$, $b_2=2e_1e_3+e_1e_2(1-w_2)-e_2^2w_2, b_3=e_1^2$, $d_1=\mu(\mu+1)e_3^2+e_2e_3\mu^2$, $d_2=2e_1e_3\mu(\mu+1)+e_1e_2\mu^2-e_2e_3-e_2^2\mu$, $d_3=e_1^2\mu(\mu+1)-e_2^2-e_1e_2$, $e_1=\alpha_2^0(3+2\alpha_2^1), e_2=6\alpha_2^1, e_3=e_1-e_2$ and $\mu=\alpha_1^1/\alpha_2^1$.

Step III: Determine the values of the parameters. First, the range of $\eta\in(\eta_{\min},\eta_{\max})$ is determined by using the constraints of $w_2(\eta,\alpha_2^0,\alpha_2^1)<1/2$ (see Fig. 1) and $\alpha_1^1(\eta,\alpha_2^0,\alpha_2^1)<1/2$ (restricted by free fall [7]) and imposing the asymptotic requirements of $\alpha_2^0=0.06$ (see the descriptions of the experiments [12,14,23]) and $\alpha_2^1=0.05$ (see other theories [8,10,22]). In fact, the fourth (third) expressions in Eq. (A2) show that w_2 (α_1^1) is a decreasing (increasing) function of η in the region near $\eta=1$, thus giving $\eta_{\min}=\eta(w_2=1/2,\alpha_2^0,\alpha_2^1)=0.56$ and $\eta_{\max}=\eta(\alpha_1^1=1/2,\alpha_2^0,\alpha_2^1)=1.37$. Second, by using the fourth and fifth expressions of Eq. (A2), one can calculate w_2 and C_{g_0} by assigning specific η to give specifically $w_2(\eta=1,\alpha_2^0,\alpha_2^1)=0.24$ and $C_{g_0}(\eta=1,\alpha_2^0,\alpha_2^1)=2.5$, a recommended value given by Dimonte [7].

Step IV: Utilize the obtained C_{g_0} to determine the drag coefficient C for the variable acceleration problem. For variable acceleration problem, a time-dependent value of $C[g(t)]$ is expected to be obtained with the main logic summarized as follows. In physics, drag is proportional to the surface area of the bubble structure [1,8] (denoted as S) and is highly dependent on the direction of mixing. For a case in which $v_2\geqslant 0$, the drag is dominated by chunk mixing near the local mixing front, and the experiments further imply a negative correlation between S and dg/dt [12,15], leading to $C=C_{g_0}$, $C\approx C_{g_0}$, $C<C_{g_0}$, $C>C_{g_0}$ for problems driven by constant, oscillating, increasing, and decreasing acceleration histories, respectively. In contrast, for cases in which $v_2<0$, the drag is dominated by atomic mixing [26] across the entire BMZ and SMZ ($S\gg S_{v_2\geqslant 0}$), leading to $C\gg C_{g_0}$.

[1] B. Cheng, J. Glimm, and D. H. Sharp, Phys. Rev. E **66**, 036312 (2002).
[2] W. H. Cabot and A. W. Cook, Nature Phys. **2**, 562 (2006).
[3] D. Livescu, Philos. Trans. R. Soc. London A **371**, 20120185 (2013).
[4] P. P. Eggleton, D. S. Dearborn, and J. C. Lattanzio, Science **314**, 1580 (2006).
[5] A. Burrows, Nature (London) **403**, 727 (2000).
[6] R. D. Petrasso, Nature (London) **367**, 217 (1994).
[7] G. Dimonte, Phys. Plasmas **7**, 2255 (2000).
[8] U. Alon, J. Hecht, D. Ofer, and D. Shvarts, Phys. Rev. Lett. **74**, 534 (1995).
[9] J. D. Ramshaw, Phys. Rev. E **58**, 5834 (1998).
[10] J. Glimm, D. Saltz, and D. H. Sharp, Phys. Rev. Lett. **80**, 712 (1998).
[11] J. Hansom, P. Rosen, T. Goldack, K. Oades, P. Fieldhouse, N. Cowperthwaite, D. Youngs, N. Mawhinney, and A. Baxter, Laser Part. Beams **8**, 51 (1990).
[12] G. Dimonte and M. Schneider, Phys. Fluids **12**, 304 (2000).
[13] B. Cheng, J. Glimm, and D. Sharp, Phys. Lett. A **268**, 366 (2000).
[14] D. L. Youngs, Physica D: Nonlinear Phenomena **37**, 270 (1989).
[15] G. Dimonte and M. Schneider, Phys. Rev. E **54**, 3740 (1996).
[16] G. Dimonte, P. Ramaprabhu, and M. Andrews, Phys. Rev. E **76**, 046313 (2007).
[17] G. Dimonte, D. Youngs, A. Dimits, S. Weber, M. Marinak, S. Wunsch, C. Garasi, A. Robinson, M. Andrews, P. Ramaprabhu *et al.*, Phys. Fluids **16**, 1668 (2004).
[18] K. R. Sreenivasan and S. I. Abarzhi, Philos. Trans. R. Soc. London A **371**, 20130267 (2013).
[19] B. Cheng, J. Glimm, D. Saltz, and D. Sharp, Physica D: Nonlinear Phenomena **133**, 84 (1999).
[20] D. L. Youngs, Philos. Trans. R. Soc. London A **371**, 20120173 (2013).
[21] Q. Zhang, Phys. Rev. Lett. **81**, 3391 (1998).
[22] U. Alon, J. Hecht, D. Mukamel, and D. Shvarts, Phys. Rev. Lett. **72**, 2867 (1994).
[23] M. B. Schneider, G. Dimonte, and B. Remington, Phys. Rev. Lett. **80**, 3507 (1998).
[24] G. Dimonte, Phys. Rev. E **69**, 056305 (2004).
[25] P. Ramaprabhu, G. Dimonte, and M. Andrews, J. Fluid Mech. **536**, 285 (2005).
[26] D. Livescu, T. Wei, and M. Petersen, J. Phys.: Conf. Ser. **318**, 082007 (2011).